Faster Diffusion across an Irregular Boundary

A. Rozanova-Pierrat[*]

Laboratoire de Physique de la Matière Condensée, C.N.R.S.-Ecole Polytechnique, 91128 Palaiseau, France
and Laboratoire de Mathématiques Appliquées aux Systèmes, Ecole Centrale Paris, 92295 Châtenay-Malabry, France

D. S. Grebenkov[†] and B. Sapoval[‡]

Laboratoire de Physique de la Matière Condensée, C.N.R.S.-Ecole Polytechnique, 91128 Palaiseau, France

We investigate how the shape of a heat source may enhance global heat transfer at short time. An experiment is described that allows us to obtain a direct visualization of heat propagation from a prefractal radiator. We show, both experimentally and numerically, that irregularly shaped passive coolers rapidly dissipate at short times, but their efficiency decreases with time. The de Gennes scaling argument is shown to be only a large scale approximation, which is not sufficient to describe adequately the temperature distribution close to the irregular frontier. This work shows that radiators with irregular surfaces permit increased cooling of pulsed heat sources.

PACS numbers: 05.60.−k, 44.05.+e, 66.10.C−

Propagation of heat as well as particle diffusion are of direct interest in everyday life, chemical industry, life sciences, and pollution spreading. In electronics or civil engineering, one needs to improve the cooling of microprocessors and build efficient radiators for housing. Empirically, a large surface is known to dissipate more so that irregularly shaped metallic radiators are placed onto microprocessors in order to remove heat. But this is the result of both conduction and convection. In this Letter, we present an experimental, theoretical, and numerical study of purely diffusive heat transfer that aims at revealing the role of the shape of the radiator.

This question has been intensively investigated in a steady state regime in which the diffusive transfer toward a boundary is governed by the Laplace equation. In this case, a general mathematical result known as the Makarov's theorem states that, in 2D, the information dimension of the harmonic measure (which describes the distribution of particles arrived onto the boundary) is strictly equal to 1 for any simply connected set, whatever the complexity of its boundary [1]. In physical terms, this means that, *contrary to intuition*, regular and irregular boundaries work similarly in the steady state regime [2–4].

In this Letter, we report the first experimental observation that regular and irregular boundaries behave differently in the transitory (or time-dependent) regime. We show that the role of irregular boundaries is important and provide quantitative explanations based on theory and numerical simulations. Note that transitory diffusion from an irregular surface has been already studied in the context of impedance spectroscopy in electrochemistry [5,6], NMR relaxation in porous media [7,8], Brownian motion near fractal surfaces [9], and heat transfer [10]. Rigorous short-time asymptotics have been reported for diffusive transfer at fractal boundaries [11–17].

We present a direct experimental visualization of heat propagation from a ''fractal'' radiator in 2D. Fractals are complex shapes that contain a large variety of geometrical feature sizes [18], and it has been already shown that deterministic and random shapes exhibiting the same fractal dimensions, behave similarly [19].

We check, for the first time, the validity of the de Gennes scaling argument [20], which is often used to understand heat propagation and diffusion from an irregular surface [5,7,21]. Relying on experimental results and numerical solutions of the underlying Fourier equation, we conclude that this argument can only be a large scale approximation which is not sufficient to describe temperature distribution close to the irregular frontier.

The heat propagation in 2D has been studied experimentally using liquid crystal temperature imaging [22,23]. The heat source is constituted by a highly conductive, 4 mm thick, aluminum sheet [Fig. 1(a)]. A complex perforation has been laser machined through this plate to obtain the third generation of the quadratic von Koch snowflake of fractal dimension $3/2$. The aluminum heat source is heated around $T_s \approx 40°$ C. It is then put on the liquid crystal plate (at temperature $T_0 \approx 20°$ C), which was set on a Styrofoam block with very small heat conductivity. This constitutes, to a good approximation, a 2D heat propagation system. A video camera monitors the time evolution of the temperature distribution by following the displacement of the visible isotherm lines imaged by their color [Fig. 1(b)–1(f)]. The entire film can be seen in the Supplemental Material [27]. At each time t, one can extract by a thresholding procedure an isotherm curve $\mathbf{r}_t$ of a given color (at temperature T). Since a quantitative measure of the heat $Q(t)$ transferred from the source from time 0 to t is not directly accessible, one has to resort to an approximation. The first guess is that $Q(t)$ is approximated
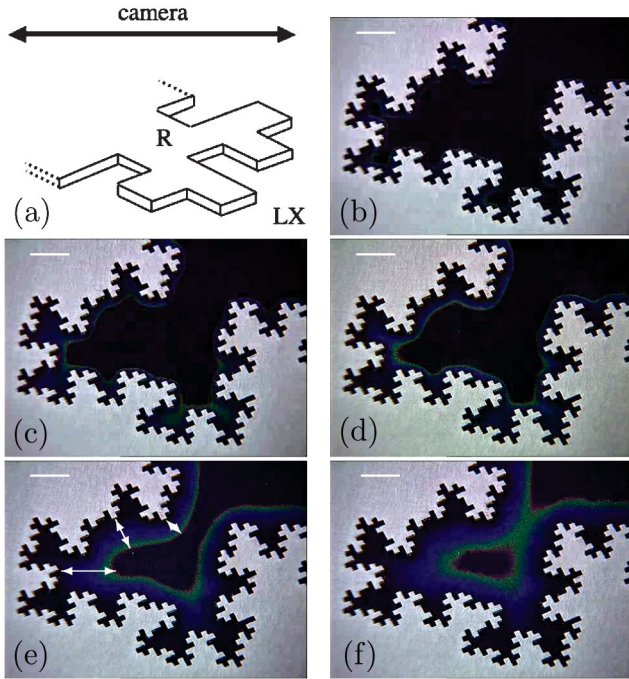
FIG. 1 (color).   Experimental visualization of heat propagation in 2D. (a) Schematic representation of the experimental setup. A 4 mm thick aluminum plate profiled following a fractal pattern is put above a liquid crystal film itself put above a thermally insulating Styrofoam layer. The large heat capacity and large thermal conductivity of the heat source assure the uniformity of the source temperature; (b)–(f) Motion of the isocolor or iso-thermal line as a function of time (at 5, 10, 20, 40, and 46 seconds, respectively). The different lengths of the white arrows in (e) illustrate the confinement effect discussed in the text. The white bar presents a length scale of 1 cm.

by the surface area $S_T(t)$ between the prefractal source and the isotherm curve $\mathbf{r}_t$:

$$Q(t) \simeq c\delta(T_s - T_0)S_T(t), \tag{1}$$

where $T_s - T_0$ is the temperature drop between the heat source and the domain, c the film specific heat and δ its thickness. The estimation of $S_T(t)$ from the experimental images is shown in Fig. 2(a) on which one observes successive power laws. In order to explain this behavior and to check the validity of the approximation (1), we recall the theoretical background, the currently admitted scaling argument, and present direct numerical simulations of heat propagation.

In the experiment, due to the very large contrast between the thermal diffusivities of aluminum and the liquid crystal film, the temperature over the aluminum sheet and at its frontier Γ can be considered as constant (T_s), imposing a Dirichlet boundary condition on the heat source. The temperature distribution $T(\mathbf{r}, t)$ over the domain (denoted as Ω) is thus the solution of the following problem [24,25]:
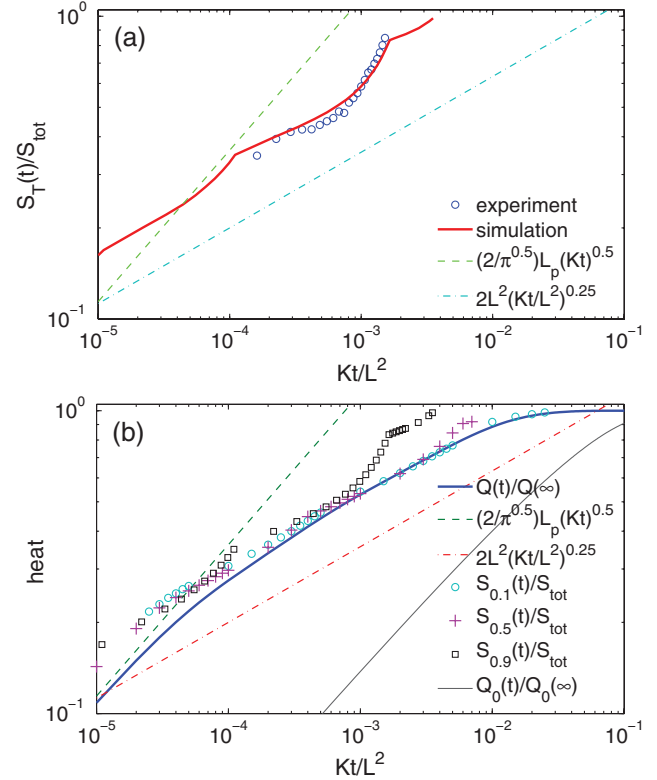

FIG. 2 (color).   Time evolution of the heat $Q(t)$ transferred from the source. (a) Evolution of the area $S_T(t)$ of the layer delimited by the visualized isotherm: experiment (circles) and numerical simulations (solid line) of the layer corresponding to the isotherm level $\theta = 0.9$ (a.u.), best fit for the experimental curve, see text. Short-time asymptotic (4) and intermediate asymptotic (5) slopes are shown by dashed lines and dash-dotted lines. (b) Numerical computation of $Q(t)$ (solid blue line) and of the three areas $S_{0.1}(t)$, $S_{0.5}(t)$, $S_{0.9}(t)$ (symbols), all computed. The curves $S_T(t)$ are shifted along the horizontal axis by factors 5, 1 (no shift), and 0.11, respectively. As explained in the text, these shifts account for the coefficient $\beta(T)$ whose dependence on the chosen isotherm level is unknown for the prefractal boundary. The thermal response $Q_0(t)/Q_0(\infty)$ of the square initiator of the same area is shown by solid black line (see Supplementary Material [27] for details). Note that $Q(t)$ and $S_T(t)$ are divided by their maximum values to be comparable.

$$\frac{\partial}{\partial t}T(\mathbf{r}, t) - K\Delta T(\mathbf{r}, t) = 0 \qquad (\mathbf{r} \in \Omega),$$
$$T(\mathbf{r}, t) = T_s(\mathbf{r} \in \Gamma), \qquad T(\mathbf{r}, t = 0) = T_0, \tag{2}$$

where Δ is the 2D Laplace operator and K the liquid crystal thermal diffusivity (of order $0.1 \text{ cm}^2\text{ s}^{-1}$). The amount of heat $Q(t)$ transferred into Ω is simply:

$$Q(t) = c\delta \int_\Omega d\mathbf{r}(T(\mathbf{r}, t) - T_0). \tag{3}$$

The fact that Eqs. (2) also describe particle diffusion suggests a random walk interpretation of the conduction experiment. In this representation, a source (here the

constant temperature T_s at radiator) is maintained at a given concentration. Its boundary emits diffusive random walkers that invade progressively the initially empty medium Ω. These walkers form a diffusion layer whose area can be tentatively used as a proxy for the transferred heat according to Eq. (1).

De Gennes suggested to replace this area by that of the so-called "Minkowski sausage" [26] of average width $l_D(t)$ taken of order $\sqrt{Kt}$ [20]. The transferred heat is then related, through Eq. (1), to the area $M(t)$ of the Minkowski sausage, $S_T(t) \simeq M(t)$, so that the heat diffusion problem is replaced by a purely geometrical computation of the area $M(t)$.

In this frame, a qualitative picture of heat propagation can be drawn from the comparison between the width $l_D(t)$ and the relevant geometrical length scales: the size l of the smallest geometrical detail of the interface (the smaller cutoff) and the size of the larger cutoff L of the boundary. For a prefractal boundary as that of the experiment, three different regimes can be expected. (i) At very short times, the diffusion width is much smaller than the smallest cutoff l and the whole interface transfers heat (or particles) almost uniformly. The area of the Minkowski sausage is then close to

$$M(t) \simeq L_p \sqrt{Kt}, \tag{4}$$

where L_p is the total perimeter of the boundary which scales as $L_p \propto l(L/l)^{d_f}$ for a surface of Minkowski dimension d_f. (ii) When the diffusion width l_D becomes comparable to l, the scaling of the Minkowski sausage behaves differently. For self-similar boundaries, the Minkowski sausage area scales with its width l_D as $l_D^{d-d_f}$, from which [20]:

$$M(t) \propto L^d (Kt/L^2)^{(d-d_f)/2}. \tag{5}$$

In our case with $d_f = 3/2$ and $d = 2$, the transferred heat is expected to follow a $t^{0.25}$ power law. This intermediate regime lasts up to the time when the diffusion length reaches the larger cutoff L of the interface. (iii) From this time, the heat transfer saturates since the domain is bounded.

Those scaling arguments should provide an explanation for the experimental power laws shown on Fig. 2. And indeed there is a regime where the surface $S_T(t)$ follows a power law with an exponent close to 0.25, but it is followed by a regime with an exponent larger than 0.5. We show now that the de Gennes argument is not sufficient to interpret the experiment because it neglects the role of confinement which might play an important role depending on the isotherm under consideration. Keeping in mind the exact correspondence with random walkers, one has to take care that the concentration of particles reaching a given point is formed by particles emitted by the several faces surrounding this point. This behavior is indicated by the white

arrows in Fig. 1(e), in which the isotherm emerging from a salient wedge is clearly much closer to the surface than the same isotherm in a confined region. In other words, the assumption of an approximately uniform diffusion layer, which could be characterized by an average width l_D, is not valid for our experiment. As a consequence, the two areas, $M(t)$ (fixed by the geometrical width l_D of the Minkowski sausage) and $S_T(t)$ (set by the isotherm of a given temperature T), are not equivalent.

An exact example illustrating this fact is given in the Supplementary Material [27], where we derive the short-time asymptotic behavior of the transferred heat and the area $S_T(t)$ for a spherical domain. In two dimensions, we get

$$Q(t) \simeq c\delta(T_s - T_0)\frac{2}{\sqrt{\pi}}L_p\sqrt{Kt},$$
$$S_T(t) \simeq 2\beta(T)L_p\sqrt{Kt}, \tag{6}$$

where $L_p = 2\pi R$. The factor $\beta(T)$ is given, for spherical domains, by $\beta = \text{erfc}^{-1}(\theta)$, where $\theta = (T - T_0)/(T_s - T_0)$ is the relative temperature of the isotherm under consideration ($\text{erfc}^{-1}(z)$ is the inverse complementary error function). Although both quantities in Eq. (6) are proportional to $L_p\sqrt{Kt}$, the quantity associated with the isotherm (i.e., $c\delta(T_s - T_0)S_T(t)$) differs from the real heat quantity that has diffused. This is due to the value of β, which can be very small if θ is close to 1, a situation corresponding to the experiment. In particular, the curves shown on Fig. 2 can only be compared up to a shift along the x or y axis, which represents a multiplication by β on logarithmic scale.

In general, the approximation (1) is expected to be more accurate for isotherms with small difference $T - T_0$ because nearly all the heat will be found inside the layer. In fact, representing Ω as $\Omega^> \cup \Omega^<$ (with $\Omega^{\lessgtr} = \{\mathbf{r} \in \Omega : T(\mathbf{r}, t) \lessgtr T\}$), the integral in Eq. (3) splits in two parts, which can be approximated at short times as

$$Q(t) \approx c\delta(T_s - T)\text{Vol}(\Omega^>) + c\delta(T - T_0)\text{Vol}(\Omega^<),$$

where the first term is close to $c\delta(T_s - T_0)S_T(t)$ for T close to T_0, while the second term can be neglected in that case. In the opposite situation, which is relevant for the experiment, the approximation (1) fails.

We illustrate this idea by solving numerically Eqs. (2) for the third generation of the quadratic von Koch curve shown in Fig. 3. The solution was obtained by the quadratic Lagrange finite differences method in the module "PDE, Coefficient Form" of COMSOL Multiphysics. The time-dependent solver for a symmetric linear system "Spooles" was used. For these simulations, we set: $T_s = 1$ (a.u.), $T_0 = 0$, $K = 0.01$ (a.u.), and $L = 1$ (a.u.) (L is the base of the snowflake curve). Once the solution $T(\mathbf{r}, t) = \theta(\mathbf{r}, t)$ is found, the isotherm curve $\mathbf{r}_t$ was computed by solving $T(\mathbf{r}_t, t) = T$ with a chosen T and then the surface area $S_T(t)$ between the isotherm and the boundary was calculated by a thresholding procedure (as for experimental images). Figure 3 shows that, at a given time, the zones
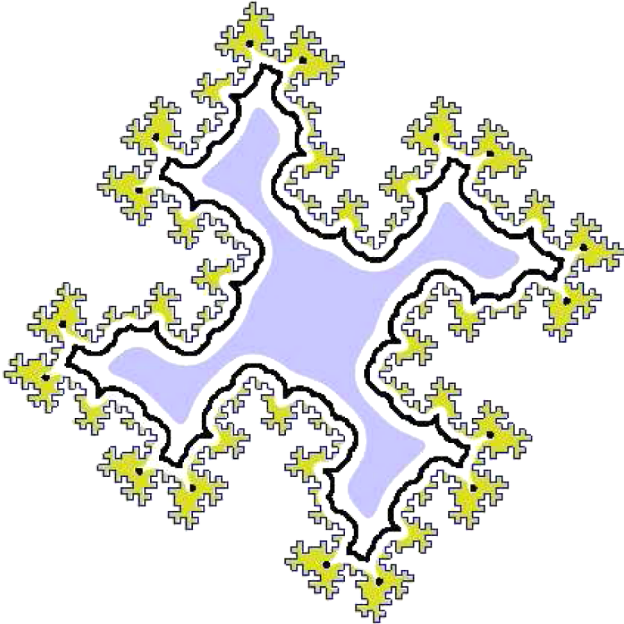
FIG. 3 (color online). Three temperature zones at $t = 0.1$ s: $\theta(\mathbf{r}, t) > 0.9$ (yellow), $0.1 < \theta(r, t) < 0.9$ (white), and $\theta(\mathbf{r}, t) < 0.1$ (blue). The frontiers between successive zones are the isotherm at $\theta = 0.9$ (a.u.) and $\theta = 0.1$ (a.u.), which are compared to the Minkowski sausage of width $\sqrt{Kt}$ (shown by the thick solid line), at $t = 0.1$ s.

defined by the isotherms depend strongly on their temperature. The relative positions of isotherms at a given time illustrate the role of confinement, observed in the experiment [Fig. 1(e)].

The total transferred heat $Q(t)$ is also obtained by integrating the solution $T(\mathbf{r}, t)$ over Ω. The results are summarized in Fig. 2(b), which shows the normalized transferred heat, $Q(t)/Q(\infty)$, and the normalized surface areas, $S_T(t)/S_{\text{tot}}$, for three choices of the isotherm temperature θ: 0.1, 0.5, and 0.9 (a.u.), together with the transferred heat into a square of the same surface. The normalization ensures that all the curves approach the same saturation level. Several comments are in order. (i) The heat transferred by the irregular radiator is larger than that by the square. (ii) The normalized transferred heat (solid curve) indeed exhibits the three scaling regimes discussed above: short-time behavior $\propto t^{0.5}$, intermediate behavior $\propto t^{0.25}$, and finally saturation. The asymptotics are shown by dashed and dash-dotted curves, respectively. (iii) Three normalized surface areas (shown by circles, squares, and triangles) have been shifted along the horizontal axis by factors 5, 1, and 0.11 in order make them follow the solid curve. These shifts (on logarithmic scale) are equivalent to the choice of the appropriate values for the coefficient $\beta(T)$. As expected, the curve with $\theta = 0.1$ shows the best agreement with the solid curve for the transferred heat, while that with $\theta = 0.9$ exhibits a strong deviation at long times. (iv) Deviations at short times can

be attributed to an inaccurate computation of the surface area $S_T(t)$ by the thresholding procedure. Although this computation could be improved for isotherms obtained from numerical simulations, the thresholding procedure remains unavoidable for experimental images. In order to be able to compare numerical and experimental images, we used the same image processing in both cases. (v) The surface area $S_T(t)$ estimated from experimental images is also shown in Fig. 2(a). This curve closely follows the numerical curve with $\theta = 0.9$. The agreement between numerical simulations and the experiment can be considered as good. This consideration is reinforced by the fact that taking care of the scale of temperature (40 to 18 centigrade) the value 0.9 corresponds to a temperature of 37.8 centigrade while the isotherm color (yellow) is calibrated for 37 centigrade. (vi) The experiment does not allow a good determination of the short-time regime because the heat propagation was faster than the time to set the camera so that the earlier times could not be monitored.

In summary, the heat transfer in an irregularly-shaped domain with a prefractal geometry has been studied experimentally and numerically. The temperature evolution has been visualized experimentally by monitoring isocolor or isothermal lines. The area of a diffusion layer between the irregular heat source and a chosen isothermal line has been computed by thresholding the sequence of recorded images. We have shown that the de Gennes suggestion to describe the diffusion layer by a Minkowski sausage and to use its area as a proxy of the total amount of heat transferred up to time t applies only to temperatures far from that of the heat source. For temperatures close to the heat source, confinement effects play an important role so that the temperature spatial distribution is very different from a Minkowski layer.

We have then shown in a particular prefractal case that irregular morphology significantly speeds up heat transfer. The ideas and concepts developed in this study apply to any irregular shape, fractal or not. This suggests that irregular or fractal shapes can be used to increase heat removal from pulsed heat sources in electronics and microelectronic devices. Depending on temperature, the phenomenon may or may not be described by the concept of a Minkowski layer. More generally, these results apply to all physical phenomena governed by the Fourier equation, such as particle diffusion, spin diffusion, and diffusion regimes in electrochemistry.

*anna.rozanova-pierrat@ecp.fr
†denis.grebenkov@polytechnique.edu
‡bernard.sapoval@polytechnique.edu

[1] N. G. Makarov, Proc. London Math. Soc. **s3-51**, 369 (1985).

[2] T. C. Halsey and M. Leibig, Ann. Phys. (N.Y.) **219**, 109 (1992).

[3] B. Sapoval, Phys. Rev. Lett. **73**, 3314 (1994).

[4] D. S. Grebenkov, M. Filoche, and B. Sapoval, Phys. Rev. E **73**, 021103 (2006).

[5] T. Pajkossy and L. Nyikos, Electrochim. Acta **34**, 171 (1989); **34**, 181 (1989).

[6] B. Sapoval, in *Fractals and Disordered Systems*, edited by A. Bunde, S. Havlin (Springer-Verlag, Berlin, 1991), pp. 207–225.

[7] B. Sapoval, S. Russ, J.-P. Korb, and D. Petit, Fractals **4**, 453 (1996).

[8] D. S. Grebenkov, Rev. Mod. Phys. **79**, 1077 (2007).

[9] P. Levitz, D. S. Grebenkov, M. Zinsmeister, K. M. Kolwankar, and B. Sapoval, Phys. Rev. Lett. **96**, 180601 (2006).

[10] D. Vandembroucq, C. Boccara, and S. Roux, Europhys. Lett. **30**, 209 (1995).

[11] C. G. Phillips and K. M. Jansons, Proc. R. Soc. A **428**, 431 (1990).

[12] J. Fleckinger, M. Levitin, and D. Vassiliev, Proc. London Math. Soc. **s3-71**, 372 (1995).

[13] M. Levitin and D. Vassiliev, Proc. London Math. Soc. **s3-72**, 188 (1996).

[14] M. van den Berg and F. den Hollander, Proc. London Math. Soc. **78**, 627 (1999).

[15] M. van den Berg, Probab. Theory Relat. Fields **118**, 17 (2000).

[16] D. Campos, V. Mendez, and J. Fort, Phys. Rev. E **69**, 031115 (2004).

[17] M. R. Lancia, Le Matematiche **67**, 271 (2007).

[18] B. Mandelbrot, *The Fractal Geometry of Nature* (Freeman & Company, New York, 1982).

[19] M. Filoche and B. Sapoval, Phys. Rev. Lett. **84**, 5776 (2000).

[20] P.-G. de Gennes, CR Acad. Sci. IIB **295**, 1061 (1982).

[21] A. Imre, T. Pajkossy, and L. Nyikos, Acta Metall. Mater. **40**, 1819 (1992).

[22] J. Stasiek, Heat Mass Transfer **33**, 27 (1997).

[23] C. R. Smith, D. R. Sabatino, and T. J. Praisner, Exp. Fluids **30**, 190 (2001).

[24] J. Crank, *The Mathematics of Diffusion* (Clarendon, Oxford, 1975), 2nd ed..

[25] H. S. Carslaw and J. C. Jaeger, *Conduction of Heat in Solids* (Clarendon, Oxford, 1959), 2nd ed.

[26] The Minkowski sausage (or ϵ-neighboring) Ω_ϵ of an arbitrary set Ω is the set of points within a distance ε to this set [18,28]. Although this term is sometimes used for the quadratic von Koch curve, this identification is erroneous and misleading.

[27] See Supplemental Material at http://link.aps.org/supplemental/10.1103/PhysRevLett.108.240602 for a direct visualization of heat transfer (movie) and for an exact solution of the heat equation in spherical and rectangular domains.

[28] M. Schroeder, *Fractals, Chaos, Power Laws* (Freeman & Company, New York, 1991).